JOURNAL OF COMPUTATIONAL PHYSICS 68, 89–103 (1987)

Numerical Solution of the Schroedinger Equation with a Non-local Exchange Kernel

DIPAK H. OZA AND JOSEPH CALLAWAY

Department of Physics and Astronomy, Louisiana State University, Baton Rouge, Louisiana 70803-4001

Received May 22, 1985; revised February 24, 1986

We describe the linear algebraic method for the numerical solution of the integral form of the Schroedinger equation with a nonlocal exchange kernel. We show explicitly the implementation of Newton–Cotes quadrature formulae of high order in order to account properly for the discontinuities arising in the derivative of the integrands originating from the two-particle Green's functions and the nonlocal kernels. The proposed technique is backed by numerical examples from scattering theory—scattering by a Yukawa potential and electron scattering by hydrogenic ions in the static-exchange approximation. The method is found to be efficient and numerically stable. © 1987 Academic Press, Inc.

1. INTRODUCTION

In the scattering of slow electrons by atoms, ions, or molecules one needs to allow for the indistinguishability of the projectile electron and the target electrons for an accurate description of the process. Mathematically, this results into a nonlocal exchange operator in the partial wave Schroedinger equation. Nonlocal operators in the partial wave Schroedinger equation occur in the scattering problem in other areas of physics involving identical Fermi particles in the projectile and the target. The complex optical potential treatment of nucleon scattering by nuclei provides such an example.

We have adapted the following approach to the solution of the integrodifferential equation. We convert the partial wave integrodifferential Schroedinger equation to an integral equation with the use of appropriate Green's functions. The integrals in the ensuing equation are approximated by discrete numerical quadratures giving us a set of linear-algebraic equations. This set of equations is solved to obtain the solutions at the designated quadrature points. This approach can be readily generalized to a multichannel scattering problem involving a set of coupled integrodifferential equations. This approach has the advantage of being noniterative in nature and is found to be numerically stable.

The basic ideas of the method were applied to study the low energy elastic scattering of thermal neutrons by deuterons a long time ago (Motz and Schwinger [1]). A careful study was performed by Fraser [2] in the late fifties;

0021-9991/87 $3.00

Fraser subsequently applied this method to the scattering of orthopositronium by hydrogen atoms [3]. The linear algebraic method has also been extensively used by Seaton's group [4] for electron–atom and electron–ion collisions. In their work, finite difference formulae are used for the differential operators on a grid of points. This gives rise to a set of linear algebraic equations for the unknown scattering functions. More recently the method has been exploited for the solution of integrodifferential equations in the integral form by Collins and Schneider [5] for electron-molecule scattering. For other representative applications of this approach, the reader is referred to the work of Ho and Fraser [6], El-gendi [7], and Stern [8, 9].

Although the linear algebraic method has been rather extensively used, some previous workers have ignored derivative dicontinuities in the Green's functions [5]. The difficulty associated with the discontinuity of the slope of the integrand was recognized by Fraser [2, 3] some time ago. Ignoring the discontinuity of the slope can produce misleading results. For example, in the test case of static-approximation of electron-hydrogen scattering (without exchange effects) examined by Stern [8], it was inferred that a low order quadrature scheme, the trapezoidal rule, is more reliable than the higher order Newton–Cotes and Gauss-quadrature schemes. This is appropriately attributed to the inadequate representation of the discontinuous derivative of the Green's function at the mesh-points in the higher order quadrature schemes (see Section 2.B). We have developed an efficient algorithm which allows for the derivative discontinuities, and enables the use of higher order Newton–Cotes formulae. In this respect, the present work is a significant advance over previous ones. We are able to treat the exchange effects (nonlocal kernels) and extension to the multichannel situation within the same framework. For improved efficiency, use of a matrix form is made for the representation of the linear operation of integration. The numerical procedures of the present approach are well adapted for implementation on vector processing computers.

In Section 2, we set up the basic equations for which we seek numerical solutions and discuss the implementation of Newton–Cotes quadrature schemes with well-defined error terms. In Section 3, we present two illustrative examples; (i) scattering of a particle by Yukawa potential where the results can be compared with the existing accurate results and (ii) scattering of electron by a hydrogenic ion in the static-exchange approximation to allow for nonlocal kernels. We follow with numerical results and our conclusions.

2. Formalism

A. *Basic Equations*

We consider the following integro-differential equation

$$[H(r) - k^2 + V(r)]\, u(r) + \int_0^\infty dx\, x^2 W(r, x)\, u(x) = 0, \tag{1}$$

where $H(r)$ is the radial Hamiltonian for which the solution of the wave- equation is known analytically. This solution would be used in the construction of the Green's function. Typically, $H(r)$ has a term with second radial derivative, an angular momentum term and perhaps a simple potential like the Coulomb potential. $V(r)$ and $W(r, x)$ are, respectively, the local (direct) and nonlocal (exchange) potentials.

We can regard Eq. (1) as describing a one-channel problem: in this case H, V, W, and u are functions; or a multichannel problem in which case $u(r)$ is a vector, $V(r)$ and $W(r, x)$ are symmetric matrices, and $H(r)$ and k^2 are diagonal matrices. For simplicity, we begin with the single channel case.

We solve (1) formally by the Green's function technique. Let $G(r, r')$ be the solution to the following equation

$$[H(r)-k^2]\, G(r, r')=\frac{\delta(r-r')}{r^2}. \tag{2}$$

In general, the two-particle Green's function can be expressed as

$$G(r, r')= -f(kr_<)g(kr_>), \tag{3}$$

where f and g are the regular and irregular solutions of the second order homogenous differential equation, and $r_<$ and $r_>$ are the smaller and the greater of r and r', respectively.

Assume that the solution $u(r)$ obeys the asymptotic boundary condition for the description of scattering, viz.

$$\lim_{r\to\infty} u(r)\sim f(kr)+\tan\delta g(kr). \tag{4}$$

It can be shown that Eq. (1) can be expressed in the integral form,

$$u(r)=f(kr)-\int_0^\infty G(r, r')\, V(r')\, u(r')\, r'^2\, dr'$$

$$-\int_0^\infty x^2\, dx\, u(x)\int_0^\infty G(r, r')\, W(r', x)\, r'^2\, dr'. \tag{5}$$

In practice, the potentials involved in Eq. (5) would generally be short- range and so the upper integration limit could be reduced to an appropriate finite value, say R.

At this point, the general practice would be to apply a numerical quadrature scheme for the integrals in (5). As long as the points of the unknown function u are the same as the pivotal points of the quadrature scheme, we have a closed system of simultaneous linear algebraic equations. The solutions of this system of equations determine the unknown function u on a grid of points corresponding to the pivotal points of the quadrature. Let us carefully examine the application of various quadrature schemes in the next subsection.

B. *Numerical Quadratures*

An integral can be approximated using a numerical quadrature scheme as

$$\int_a^b y(x)\,dx = \sum_{i=1}^{N} \omega_i y(x_i) + \text{Error term.} \tag{6}$$

The order of the error term depends on the quadrature scheme used. But in order for the error term to be defined usefully, the integrand $y(x)$ must be continuous over the closed interval $[a, b]$ and differentiable m times over the open interval (a, b), where m depends on the specific order of approximation for the quadrature. This is due to the fact that the error term is evaluated by the application of the mean-value theorem.

In Eq. (5), the integrand contains the Green's function which has a discontinuous first derivative at $r = r'$. Also the nonlocal kernel W could have a discontinuous derivative at $r' = x$. (See our Example B.) Hence as it stands, the application of a numerical quadrature as in (6) over the full integration range would give rise to an undefined error. Fraser [2, 3] and Stern [8] have recognized this difficulty. Ho and Fraser [6] have stated in their work that they have taken due note of the discontinuities of the slope of the Green's functions without giving any details. In addition, El-gendi proposed a method using a Clenshaw–Curtis type of quadrature formula at Chebyshev points to solve integral equations containing a kernel with a discontinuous first derivative within the range of integration [7]. Stern has tried this approach for the scattering of electrons by hydrogen atoms in the static approximation, i.e., without a nonlocal exchange kernel [9]. However, Stern found that the method is inefficient in terms of computational time in comparison to the composite trapezoidal rule, the lowest order of Newton–Cotes schemes. Here we show explicitly how the difficulty associated with the discontinuous slope of the integrand within the range of integration can be overcome in the implementation of high order quadrature schemes.

We allow the points of discontinuous derivatives to be the endpoints for subranges of integration. With this in mind, we rewrite Eq. (5) as

$$\begin{aligned} u(r) = f(kr) &- \int_0^r G(r, r')\, V(r')\, u(r')\, r'^2\, dr' \\ &- \int_r^R G(r, r')\, V(r')\, u(r')\, r'^2\, dr' \\ &- \int_0^R dx\, x^2 u(x) \Bigg[\int_0^{l_<} G(r, r')\, W(r', x)\, r'^2\, dr' \\ &+ \int_{l_<}^{l_>} G(r, r')\, W(r', x)\, r'^2\, dr' \\ &+ \int_{l_>}^R G(r, r')\, W(r', x)\, r'^2\, dr' \Bigg] \end{aligned} \tag{7}$$

where $l_<$ and $l_>$ are the lesser and the greater of x and r, respectively.

The integrands for the inner integrals in the last term in (7) involving the Green's function and the nonlocal potential are specified numerically. So the integrations may be performed by any quadrature scheme. The use of unevenly spaced quadrature schemes, such as Gauss-quadratures, would be awkward. Evenly spaced quadrature formulas, such as Newton–Cotes, are relatively straightforward to implement because the values of the integrands need to be calculated once and stored. The procedure, to implement efficiently higher-order Newton–Cotes schemes for these integrals, is described here.

One needs to exercise caution with the integrals which involve the unknown function u. In order to obtain a closed set of simultaneous equations, the pivotal points of the quadrature should match the values of r on the left-hand- side, which also happens to be an endpoint in the integrals. This eliminates the use of Gauss-quadrature schemes as it would give us an underdetermined set of simultaneous equations. Even for the schemes with evenly spaced points (such as Newton–Cotes) one needs to exercise caution for the following two reasons: (1) For N-point scheme, with N other than 2, r could fall at a pivotal point between 1 and N. In this case the $\int_0^r$ integrand would need a different set of weights than the case where r falls at either 1 or N. (2) Because our potentials, V and W, may be changing very rapidly in some regions (such as exponentially varying), we would need to implement a finer mesh of evenly spaced points in those regions. We explain these two points with the help of Figure 1 below.

First, let us specify the 5-point Newton–Cotes formulae.

$$\int_{x_0}^{x_4 = x_0 + 4h} y(x)\,dx = \frac{4h}{90}\,[7y_0 + 32y_1 + 12y_2 + 32y_3 + 7y_4] + O(h^7) \qquad \text{Bode's Rule} \tag{8}$$

For smaller integration intervals (see[10]), we use

$$\int_{x_0}^{x_0 + h} y(x)\,dx = \frac{h}{720}\,[251y_0 + 646y_1 - 264y_2 + 106y_3 - 19y_4] + O(h^7), \tag{9}$$

$$\int_{x_0}^{x_0 + 2h} y(x)\,dx = \frac{h}{90}\,[29y_0 + 124y_1 + 24y_2 + 4y_3 - y_4] + O(h^7) \tag{10}$$

$$\int_{x_0}^{x_0 + 3h} y(x)\,dx = \frac{3h}{80}\,[9y_0 + 34y_1 + 24y_2 + 14y_3 - y_4] + O(h^7). \tag{11}$$

The functions with discontinuous derivatives in Eq. (7) are of the form

$$f(r)\,g(r') \qquad \text{for} \quad r \leqslant r'$$

and

$$g(r)\,f(r') \qquad \text{for} \quad r' < r,$$

where f and g are separately differentiable. The integrals actually performed using Eqs. (8)–(11) involve f or g separately, and thus no discontinuous derivatives occur in the range from x_0 to x_4.

We deal with the composite form of the 5-point Newton–Cotes closed-type formulae as follows. One of the minor restrictions in this case would be that the mesh-size must change at a $4n+1$ point and that the last point of integration must also be $4n+1$, for n a positive integer. The endpoint of an integral in Eq. (7) could fall on any of the points shown in Fig. 1. For the endpoint on points 1, 5, 9, and 13 a straightforward implementation of the composite form of Bode's rule Eq. (8), is possible with the different values of h for points below point 9 and above point 9.

For endpoints of integration falling on the other points in the figure, we have to use the appropriate quadrature given by Eq. (9), (10), or (11). It should be pointed out that the functional form of $y(x)$ for x less than the upper limit of integration is used beyond the upper limit of integration. For example, for the endpoint of integration on point 2, the integral $\int_1^2$ would be evaluated by the use of Eq. (9). Here the values of y_2, y_3, and y_4 are obtained using the same function $y(x)$ which is used to obtain values for y_0 and y_1, i.e., in application to Eq. (7), we extend the known functional form of the integrand to y_2, y_3, and y_4 in order to use Eq. (9) despite the fact that the actual values of the integrand at y_2, y_3, and y_4 would be different due to the derivative discontinuity at x_0+h. Then for $\int_2^5$ range, we would use Eq. (8) for $\int_1^5$ and (9) for $\int_1^2$ and take the difference or use (11) backwards for $\int_5^2$. Again, the values of the integrand used are extended beyond the range of integration using a single known function $y(x)$.

This explains why the mesh-size can not be changed at any arbitrary point. This procedure maintains the order of the error term to be h^7. Lower order formulas lead to somewhat simpler codes but have larger error terms ($O(h^3)$ for the trapezoidal rule, $O(h^5)$ for Simpson's rule).

For example, if in (9),

$$y(x) = f(r)\, g(x), \qquad x \leqslant x_0 + h,$$
$$= g(r)\, f(x), \qquad x \geqslant x_0 + h,$$

then the values of all the y_i on the right-hand side in (9) are obtained from $f(r)\, g(x)$ alone, even for y_2, y_3, and y_4.

We note in Eq. (7) that we require a number of integrals with different sets of endpoint values. Since integration is a linear operation, we find it convenient to represent it in the following matrix form.

$$\int_0^r y(x)\, dx = \sum_j \omega_1(i, j)\, y_j, \tag{12}$$

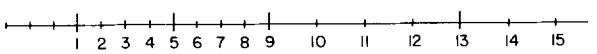

FIG. 1. An example of grid- points used in 5-point Newton–Cotes quadrature formula.

where the index i represents point r and j represents x. Similarly, we define another matrix

$$\int_r^R y(x)\,dx = \sum_j \omega_2(i,j)\,y_j. \tag{13}$$

For any arbitrary endpoints r_1 and r_2 within the closed interval 0 to R, we have

$$\begin{aligned}\int_{r_1}^{r_2} y(x)\,dx &= \sum_j [\omega_1(i_2, j) - \omega_1(i_1, j)]\,y_j \\ &= \sum_j [\omega_2(i_1, j) - \omega_2(i_2, j)]\,y_j.\end{aligned} \tag{14}$$

The matrices ω_1 and ω_2 are constructed from the number of mesh- points, mesh-sizes and the weight functions in the respective quadratures. The integrand and its necessary extensions beyond the endpoint of integration are contained in y. So once the mesh details and the quadrature are fixed, ω_1 and ω_2 matrices can be calculated one time and then used repeatedly in any number of integrals.

After the quadrature scheme has been implemented, Eq. (7) can be rewritten as

$$u(r_i) = f(kr_i) - \sum_j B_{ij} u(r_j), \tag{15}$$

where the elements of the square matrix B embody the details of the potentials, Green's functions and the quadrature scheme. It can be recast in a matrix form as

$$[\mathbf{I} + \mathbf{B}]\,\mathbf{u} = \mathbf{f}, \tag{16}$$

where $\mathbf{I}$ is the identity matrix. Our solution vector $\mathbf{u}$ can be obtained by a matrix inversion.

After knowing the solution u on the given grid-points, one can substitute it in the summation on the right-hand- side of Eq. (15) in order to have an interpolation formula to obtain $u(r)$ at any arbitrary value of r.

The present method casts the numerical work in the form of a solution to a matrix equation. This is particularly amenable to vector processing computers for a rapid numerical solution.

3. Examples

For the purpose of illustration of the method described in the previous section, we present two physical examples. The first deals with the scattering of a particle by a Yukawa potential. This example does not involve a non-local kernel. We chose this example because numerically accurate results exist [11] with which we can compare the convergence of the results of the present method. The second example is that of the scattering of electrons by hydrogenic ions in the static-exchange

approximation. This example illustrates the use of the method with a non-local potential, viz. the exchange potential. Stern [8] had examined the numerical stability of different methods for the electron scattering by hydrogen atom in the static approximation which does not include exchange. Realistic multichannel scattering calculations have been succesfully carried out using the ideas presented here [12].

A. *Scattering by Yukawa Potential*

We consider the scattering in the S-wave ($L=0$). So we have in (1),

$$H(r) = -\frac{1}{r^2}\frac{d}{dr}(r^2\frac{d}{dr}), \tag{17}$$

$$V(r) = -g^2\frac{e^{-\mu r}}{r}, \tag{18}$$

$$W(r, x) = 0. \tag{19}$$

In this case the Green's function in (3) is

$$G(r, r') = \frac{\sin(kr_<)\cos(kr_>)}{kr_<r_>}, \tag{20}$$

where $\sin kr/\sqrt{k}\,r$ and $\cos kr/\sqrt{k}\,r$ are, respectively, the regular and irregular solution of the homogenous differential equation in (2), viz.

$$\left[-\frac{1}{r^2}\frac{d}{dr}r^2\frac{d}{dr} - k^2\right] y(r) = 0. \tag{21}$$

In the asymptotic limit, the solution $u(r)$ behaves as

$$\lim_{r\to\infty} u(r) \sim \sin kr/\sqrt{k}\,r + \tan\delta\cos kr/\sqrt{k}\,r, \tag{22}$$

where δ is the phase-shift. The numerical solution at large r is matched with (22) to extract the phase-shift. Alternatively, and formally equivalently, one may also compute $\tan\delta$ by an integration over the numerically obtained wave functions [2, 8].

B. *Scattering of Electron by Hydrogenic Ion*

We consider the scattering of an electron with charge, e, by a hydrogenic ion with nuclear charge Ze in the static exchange approximation for an arbitrary partial wave. Then in (1), we have

$$H(r) = -\frac{1}{r^2}\frac{d}{dr}\left(r^2\frac{d}{dr}\right) + \frac{L(L+1)}{r^2} - \frac{(Z-1)e^2}{r}, \tag{23}$$

the direct static interaction potential is

$$V(r) = -e^2 e^{-2Zr}\left(\frac{1}{r} + Z\right) \tag{24}$$

and the exchange potential with nonlocal character is

$$W(r, x) = (-1)^S R_{1s}(r)\left[(E_{1s} - k^2)\,\delta_{L0} + \frac{e^2}{2L+1}\frac{r_<^L}{r_>^{L+1}}\right] R_{1s}(x). \tag{25}$$

In the above expressions, $R_{1s}(r)$ is the radial eigenfunction of the ground state of the hydrogenic ion, E_{1s} is its ground state energy and δ_{L0} is a Kronecker delta. The symbols $r_<$ and $r_>$ represent the smaller and the larger of r and x, respectively. S is the total spin of the system.

We use atomic units with energies in Rydbergs. We have $e^2 = 2$ and the ground state radial eigenfunction is

$$R_{1s}(r) = 2Z^{3/2} e^{-Zr}. \tag{26}$$

The solution $u(r)$ must satisfy the boundary conditions

$$\begin{aligned} ru(r) &\sim r^{L+1} && \text{for} \quad r \to 0 \\ &\sim F_L(kr) + \tan\delta G_L(kr) && \text{for} \quad r \to \infty. \end{aligned} \tag{27}$$

Here $F_L(kr)$ and $G_L(kr)$ are regular and irregular Coulomb-functions corresponding to a charge of $(Z-1)$. For hydrogen $(Z=1)$, they reduce to spherical Bessel and spherical Neumann functions. The Green's function is expressed in terms of these functions as

$$G(r, r') = -\frac{1}{k}\frac{F_L(kr_<)\,G_L(kr_>)}{r_< r_>}. \tag{28}$$

From the numerical solution $u(r)$, the phase-shifts are extracted by matching with asymptotic solution at large r, Eq. (27), as in the case of Yukawa potential.

4. Numerical Results

We have developed FORTRAN programs to generate ω_1 and ω_2 matrices defined in Eqs. (12) and (13) based on the Newton–Cotes quadrature schemes. Using these matrices, we generate the B matrices for the physical examples considered here. For the purpose of the solution of the linear algebraic equations (16), we use the subroutines from IMSL library [13]. All the computational work is performed on an IBM 3081 computer in double precision arithmetic (64 bit word).

TABLE I.

Three Different Even-Spaced Grids Used in This Work

Mesh size (h_i)	0.12	0.30	0.8		
Upto point (N_i)	9	17	25		
With radial value (r_i)	0.96	3.36	9.76		
Meth size (h_i)	0.05	0.10	0.2	0.4	0.6
Upto point (N_i)	13	17	21	33	41
With radial value (r_i)	0.6	1.0	1.8	6.6	11.4
Mesh size (h_i)	0.05	0.1	0.2	0.3	0.4
Upto point (N_i)	13	21	33	45	57
With radial value (r_i)	0.6	1.4	3.8	7.4	12.2

We give the different numerical grids used in the calculations in Table I. The meshes are chosen to be finer in the inner radial distances where the interactions are the strongest. The numerical grids used in the present work were established in most part on physical grounds, i.e., considering the range of short-range interactions. No extensive search was made for an "optimum" grid.

A. *Scattering by Yukawa Potential*

The Yukawa potential (18) is specified by $g^2 = 2.0$ and $\mu = 1.0$ for which highly accurate numerical values of the phase-shift are given by Callaway [11] at a number of energies. The calculation is performed using three different Newton–Cotes schemes. The sets of grid-points used from Table I are with a total of 25, 41, and 57 points.

The numerical values of the phase-shifts thus obtained are given in Table II. For the sake of comparison, the so-called exact phase-shifts from reference [11] are also included. With the exact values in there, the convergence patterns of various methods can be readily judged. There are really no surprises in the results. The results are much better at lower energies and deteriorate gradually with increasing energy. As the energy increases, the solution has more oscillations and thus demands a finer grid for improvement in the results. For a given number of points, with the same grid, the accuracy is significantly improved with the higher order scheme. Again for a given quadrature scheme, the finer the grid, the higher is the accuracy. Within different schemes, at the lowest energy, we observe that the phase-shift with relatively crude mesh of 25 points but with a high order 5-point Newton–Cotes scheme yields a better phase-shift than the grid of 57 points used on the 2-point Newton–Cotes scheme (trapezoidal rule). Naturally, this speaks in the favor of using the higher order schemes if they are available and can be implemented accurately. One must bear in mind that we have been able to achieve this by properly accounting for the discontinuity in the derivative of the integrand.

In order to show how a higher order scheme fails to achieve reliable and desired

TABLE II

Phase-Shifts in Radians for Scattering from Yukawa Potential for $L = 0$

	Energy	0.01	0.1	1.0	2.0	5.0	10.0
a	25	2.444589	1.726090	1.094994	0.935066	0.739757	0.603974
b	25	2.439295	1.721895	1.092177	0.933445	0.744652	0.619742
c	25	2.439522	1.721879	1.092358	0.933238	0.743034	0.621848
a	41	2.452692	1.733826	1.097427	0.935870	0.746969	0.615502
b	41	2.439975	1.722499	1.092718	0.933757	0.743640	0.619990
c	41	2.439678	1.722232	1.092477	0.933596	0.743445	0.620729
a	57	2.446079	1.727806	1.094429	0.934297	0.746887	0.618312
b	57	2.439742	1.722299	1.092544	0.933514	0.744038	0.617878
c	57	2.439662	1.722215	1.092456	0.933438	0.744341	0.617987
Exact		2.439659	1.722210	1.092461	0.933515	0.745045	0.621987
d	48	2.452020	1.733215	1.098572	0.938664	0.748490	0.620955
d	96	2.442797	1.724979	1.093983	0.934744	0.745287	0.618213
d	144	2.441058	1.723444	1.093130	0.934016	0.744693	0.617707
d	192	2.440447	1.722905	1.092831	0.933760	0.744485	0.617530
Exact		2.439659	1.722210	1.092461	0.933515	0.745045	0.621987

Note. Energy is in Rydbergs; 25, 41 and 57 are the total number of points for (a) trapezoidal rule, (b) Simpson's rule and (c) 5-point Newton–Cotes quadrature. See Table I for the numerical grid. Also included are the results with (d) Gauss–Legendre quadrature with 48, 96, 144, and 192 points. The exact phase-shifts are from [11].

accuracy if we do not explicitly account for the discontinuity in the derivative of the integrands, we have done the same calculation with Gauss–Legendre quadrature schemes of different orders. These are also given in Table II along with the exact results. The maximum radial distance we choose to go out is 12 atomic units, i.e., $R = 12.0$. From the results of the Newton–Cotes quadrature schemes, this should be sufficiently far. We observe, in the phase-shifts at $k^2 = 0.01$ Ry, that the results with quadratures up to 48 points (which is a very high order scheme) are inferior to all results using Newton–Cotes schemes. And even with a 192-point Gauss–Legendre scheme, the phase-shifts haven't achieved the accuracy of the results by Simpson's rules or the 5-point Newton–Cotes rules with the crudest of mesh-points. At large energies, such as above 2.0 Ry, the phase-shift using the increasing order of Gauss-quadrature schemes are clearly converging to an incorrect result. Similar irregularities, to a much lesser degree, also exist for the results in the Newton–Cotes schemes. But it should be borne in mind that at the highest energies the limitations are dictated by the fineness in the grid- points due to rapid radial oscillations in the solution as opposed to the adequacy of a given scheme. And so it is best to draw conclusions from the low-energy results.

We conclude from the results that the linear-algebraic method used with the integral form of the equations is numerically very stable.

B. *Scattering of Electron by Hydrogenic Ions*

The results presented here are in the static-exchange approximation. First, we present the results for the scattering of electron by the neutral hydrogen atom. The results are given for the partial waves ^1S, and ^3P, at a number of incident energies in Table III. Again as in the Yukawa potential case, we have examined three different Newton–Cotes quadrature schemes using grid- points with 25, 41, and 57 points from Table I. Such an analysis is repeated here to demonstrate that the inclusion of exchange does not cause any complications, particularly of numerical nature. Again there are really no surprises. The choice of grid- points affects the

TABLE III

Phase-Shifts in Radians for Electron Scattering by Hydrogen Atom in Static Exchange Approximation at a Number of Incident Energies (Ry)

	Energy	0.01	0.09	0.25	0.49	0.76	1.0	2.0	5.0
Singlet *S*-wave									
a	25	2.4013	1.5175	1.0365	0.7472	0.6045	0.5418	0.4893	0.5393
b	25	2.3984	1.5132	1.0306	0.7415	0.6022	0.5443	0.5116	0.5450
c	25	2.3988	1.5132	1.0307	0.7412	0.6015	0.5433	0.5104	0.5427
a	41	2.3934	1.5055	1.0276	0.7416	0.6010	0.5432	0.5128	0.5453
b	41	2.3969	1.5093	1.0308	0.7440	0.6020	0.5427	0.5096	0.5425
c	41	2.3970	1.5093	1.0309	0.7441	0.6022	0.5430	0.5096	0.5442
a	57	2.3957	1.5078	1.0304	0.7435	0.6008	0.5415	0.5078	0.5449
b	57	2.3964	1.5085	1.0311	0.7443	0.6018	0.5428	0.5094	0.5451
c	57	2.3964	1.5085	1.0311	0.7443	0.6018	0.5428	0.5093	0.5450
Triplet *P*-wave									
a	25	0.0022	0.0520	0.1732	0.2897	0.3453	0.3635	0.3609	0.3242
b	25	0.0022	0.0510	0.1695	0.2835	0.3393	0.3585	0.3598	0.3187
c	25	0.0022	0.0510	0.1693	0.2832	0.3387	0.3579	0.3597	0.3200
a	41	0.0022	0.0513	0.1702	0.2850	0.3414	0.3612	0.3648	0.3227
b	41	0.0022	0.0511	0.1694	0.2833	0.3388	0.3579	0.3593	0.3198
c	41	0.0022	0.0511	0.1693	0.2833	0.3388	0.3579	0.3594	0.3196
a	57	0.0022	0.0512	0.1698	0.2840	0.3396	0.3588	0.3606	0.3211
b	57	0.0022	0.0511	0.1694	0.2833	0.3388	0.3579	0.3594	0.3192
c	57	0.0022	0.0511	0.1694	0.2833	0.3388	0.3579	0.3594	0.3192

Note. 25, 41 and 57 are the total number of grid points for trapezodial rule (a), Simpson's rule (b) and 5-point Newton Cotes quadrature (c).

convergence more than does the order of the quadrature scheme. As a matter of fact, with the 57-point grid, the phase-shifts with the Simpson's scheme are in complete agreement with the ones with the 5-point Newton–Cotes scheme.

At the lowest incident energies, phase-shifts are significant only in S-waves. With increasing energies higher partial waves also contribute significantly to the phase-shifts. For the partial-waves presented here, our phase-shifts are in agreement with the ones reported by Burke *et al* [14] for the common incident energies of $k^2 = 0.01$, 0.09, 0.25, and 0.49 Ry. At higher energies, the scatter in our S-wave phase-shifts by different quadratures and the different grid- points is somewhat more than at the low energies. This indicates the need to improve the grid- points at higher energies due to increasing radial oscillations in the solution. For higher partial waves, the 57-point grid seems to be adequate even at $k^2 = 5.0$ Ry.

We comment here on the execution time for different cases. The c.p.u. seconds are reported for an IBM 3081 computer. For a given number of points, the execution time was found to be independent of the quadrature scheme and independent of the partial wave. This encourages us to implement higher order quadrature schemes at no extra cost. The composite c.p.u. time for the calculation of the phase-shifts at eight incident energies was found to be 1.90, 7.5, and 20.4 seconds with the grid-points having 25, 41, and 57 points, respectively. The ratios of the c.p.u. times are approximately proportional to the ratio of the cubes of the dimensions of the resulting matrices. Since it is well- known that the order of operations in the solution of a linear algebraic system is n^3 where n is the dimensionality of the system, we infer that most of our c.p.u. time is spent in obtaining the solution of the linear algebraic equations.

In Table IV, we present the phase-shifts for the scattering of electrons by hydrogenic ions with the nuclear charge of $Z = 2$ (He^+) in the static-exchange approximation. The 5-point Newton–Cotes scheme with the 57-point grid was used. The radial meshes are scaled by a factor of $(1/Z)$ to recognize the fact that with the increasing nuclear charge, the effective region of interaction shrinks in the scaled

TABLE IV

Phase-Shifts for Electron Scattering by Hydrogen-Like Helium Ion in Static-Exchange Approximation at a Number of Incident Energies (Ry)

L	S	Energy 0.04	0.36	1.0	1.96	3.04	4.0	8.0	20.0
0	0	0.3825	0.3566	0.3231	0.2996	0.2910	0.2897	0.2941	0.2859
0	1	0.9157	0.8805	0.8165	0.7387	0.6727	0.6273	0.5101	0.3765
1	0	3.0674	3.0628	3.0638	3.0770	3.0965	3.1137	0.0260	0.0881
1	1	0.1791	0.1962	0.2125	0.2179	0.2152	0.2107	0.1923	0.1647
2	0	3.1399	3.1379	3.1347	3.1320	3.1317	3.1330	0.0024	0.0320
2	1	0.0031	0.0072	0.0154	0.0264	0.0359	0.0424	0.0582	0.0725

Note. Five-point Newton–Cotes quadrature is used with a numerical grid of 57 points.

proportion. Also to keep in proportion with the energy spectrum of the target ion, the incident energies are scaled by the factor of Z^2. By a parallel calculation with the Simpson's rule (not presented here), identical phase-shifts are obtained; indicating that the reported phase-shifts have converged.

Again we observe as in the case of the Yukawa potential that the method is numerically stable.

5. Conclusions

We have described the linear algebraic method for the solution of the Schroedinger equation with a nonlocal kernel. The difficulty of encountering discontinuities in the derivatives of the integrands, due to two-particle Green's function and nonlocal exchange kernels, is recognized. A technique to implement the high order Newton–Cotes quadrature scheme with error of $O(h^7)$ in order to properly account for such discontinuities is presented. The linear operation of integration is represented in matrix form for better efficiency in handling a large number of integrals.

The practical applications of the method are demonstrated by two physical examples of increasing amount of complexity. The simplest case treated is that of the scattering of a particle by Yukawa potential. By the use of Gauss–Legendre schemes, with which it is not possible to account adequately for the aforementioned discontinuities, we show superior convergence of our technique with even-spaced Newton–Cotes quadrature schemes. It is observed that the method is somewhat tolerant to the inadequacies in the use of Gauss–Legendre schemes thereby yielding reasonable, although not very accurate, results. In problems for which the correct answers are not known ahead of the attempted solution, this fact can unfortunately lead to deceptive conclusions.

The case of the electron scattering by hydrogenic ions in the static-exchange approximation which involves nonlocal exchange kernels is also succesfully treated within the same framework. The convergence of the phase-shifts with respect to numerical grids and different quadrature schemes is examined. Phase-shifts are presented for the partial waves, ^1S and ^3P, for the one electron targets of neutral hydrogen atom and singly ionised helium ion for a number of incident electron energies.

We conclude from these example that the linear algebraic method is numerically very stable. In addition it is noniterative in nature and yields high-accuracy results. We are now using this procedure in multichannel calculations with energy-dependent, complex, nonlocal optical potentials for the scattering of electrons by hydrogen atoms and hydogenic ions [12].

Acknowledgments

The authors are indebted to Professor P. A. Fraser for providing a copy of his unpublished report [2]. This work was supported in part by the United States National Bureau of Standards.

REFERENCES

1. L. MOTZ AND J. SCHWINGER, *Phys. Rev.* **58**, 26 (1940).
2. P. A. FRASER, Scientific Report No. 4 Contract No. AF 19(604) 1718, Department of Physics, University of Western Ontario, 1958 (unpublished).
3. P. A. FRASER, *Proc. Phys. Soc.* **78**, 329 (1961).
4. M. J. SEATON, *J. Phys. B: At. Mol. Phys.* **7**, 1817 (1974); M. A. CREES, M. J. SEATON, AND P. M. H. WILSON, Comput. Phys. Comm. **15**, 23 (1978) and references therein.
5. L. A. COLLINS AND B. I. SCHNEIDER, *Phys. Rev. A* **24**, 2387 (1981) and references therein.
6. Y. K. HO AND P. A. FRASER, *J. Phys. B: At. Mol. Phys.* **9**, 3213 (1976).
7. S. E. EL-GENDI, *Comput. J.* **12**, 282 (1969).
8. M. S. STERN, *J. Comput. Phys.* **25**, 56 (1977).
9. M. S. STERN, *J. Comput. Phys.* **28**, 122 (1978).
10. A. BURGESS, D. G. HUMMER, AND J. A. TULLY, *Philos. Trans. Roy. Soc. London* **226**, 225 (1970).
11. J. CALLAWAY, *Phys. Lett. A* **77**, 137 (1980).
12. D. H. OZA AND J. CALLAWAY, *Phys. Rev. A* **32**, 2534 (1985); J. CALLAWAY AND D. H. OZA, *Phys. Rev. A* **32**, 2628 (1985).
13. International Mathematical and Statistical Library Inc., Houston Texas, 1982.
14. P. G. BURKE, D. F. GALLAHER, AND S. GELTMAN, *J. Phys. B: At. Mol. Phys.* **2**, 1142 (1969).